Nanoscale Advances

ROYAL SOCIETY OF CHEMISTRY

PAPER

View Article Online
View Journal | View Issue

Cite this: *Nanoscale Adv.*, 2021, **3**, 5650

Conjugated polymer coating enabled light-resistant black phosphorus with enhanced stability†

Xingyun Li,[ab] Bin Han,[c] Yaojie Xu,[d] Xiao Liu,*[ab] Chunhui Zhao[d] and Jun Xu *[abc]

Received 30th May 2021
Accepted 7th August 2021

DOI: 10.1039/d1na00403d

rsc.li/nanoscale-advances

As an advanced two-dimensional (2D) material with unique properties, black phosphorus (BP) has attracted great attention in a variety of fields. One of the main obstacles for the practical application of BP is the poor ambient stability of few-layer BP, especially under light irradiation. In this study, a light-absorbing conjugated polymer is functionalized on the surface of BP during the exfoliation process, yielding BP nanosheets with light-resistance. The obtained BP/polymer nanosheets demonstrate enhanced stability compared to pure BP under sunlight. Systematic characterization reveals that the crystal structure and electronic characteristics of BP are well retained after 30 days of sun exposure. This convenient and efficient conjugated polymer passivation provides a novel light-prohibited method to improve the stability of BP for future applications.

Introduction

Black phosphorus (BP), one of the latest members among various two-dimensional (2D) nanomaterials, has received extensive research interest for its unique electronic properties since early 2014.[1,2] In contrast to other well-known 2D materials (such as graphene and transition metal dichalcogenides),[3,4] BP is a semiconductor with a layer-dependent direct bandgap ranging from 0.3 to 2.0 eV.[5,6] Besides, BP possesses a large on/off ratio (up to 10^5) and excellent carrier mobility (1000 $cm^2 V^{-1} s^{-1}$).[7,8] Due to these promising properties, BP has been considered as an appealing material for sensing, energy storage, water splitting and electronic devices.[9–13]

However, bare BP nanosheets are extremely sensitive to air and quickly degrade within a few hours, especially under light irradiation, which results in the rapid loss of semiconducting properties.[14,15] While the exact mechanism of BP degradation under ambient conditions is still unclear, significant progress has been made both experimentally and theoretically. Initially, several reports pointed out that water and oxygen were the main factors in BP degradation, but parallel research works implied that light played a vital role and had a negative effect.[16–19] Light, as a trigger factor of BP degradation, could activate electrons transferring from the conduction band of BP to the O_2 and generate reactive oxygen species (ROS), which could further react with the BP surface.[17,18,20]

In order to protect BP from chemical degradation, several strategies have been developed over the years, including chemical passivation and physical encapsulation. However, those methods still have several limitations. For instance, the covalent functionalization of BP would inevitably introduce structural defects and alter the intrinsic properties of BP.[14,21,22] Instead of covalent bonding, metal ions could passivate BP by chemical adsorption, yet the protection lasting period would not be too long.[23,24] As for physical protection, while inorganic deposition layers (such as AlO_x, SiO_2, and graphene) served as physical barriers for isolating BP from oxygen and water, the layers also formed charge transport barriers and caused a dramatic decrease of conductivity.[25–27] Hence, in order to produce BP with better stability and maintain its superior properties, a more suitable strategy is to employ conductive passivation coatings which could hinder light-activated ambient degradation.

To achieve this strategy, conjugated polymers are great candidates due to their excellent conductivity and light absorbing properties.[28] The light absorbing range of conjugated polymers depends on the molecular design and conjugation length. Therefore, conjugated polymers are appropriate to be efficient light barriers for BP, which can impede photo-oxidative damage on the BP surface. The functionalization is attributed to the donor–acceptor interaction between BP and the conjugated polymer. The P atom in the BP structure has a residual lone pair of electrons, indicating that BP can serve as an electron donor to

[a]Department of Biomaterials, College of Materials, Xiamen University, Xiamen 361005, China

[b]Shenzhen Research Institute of Xiamen University, Shenzhen 518057, P. R. China. E-mail: xujun@xmu.edu.cn; liuxiao0337@163.com

[c]Department of Physics, Research Institute for Biomimetics and Soft Matter, Fujian Provincial Key Laboratory for Soft Functional Materials, Xiamen University, Xiamen, 361005, China. E-mail: xujun@xmu.edu.cn

[d]School of Materials Science and Engineering, Nanchang Hangkong University, Nanchang 330063, Jiangxi, China

† Electronic supplementary information (ESI) available. See DOI: 10.1039/d1na00403d

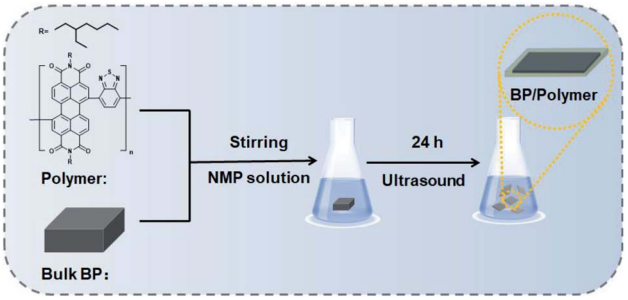

Scheme 1 Schematic illustration of the functionalization of a light-absorbing conjugated polymer on the BP surface.

provide electrons. Conversely, the conjugated polymer has a strong electron-withdrawing ability with two O=C–N–C=O groups attached to the opposite ends of a perylene core. The conjugated polymer coating layer offers the following advantages: (1) the broad light absorption region (from the ultraviolet to the visible region) can greatly reduce the light induced oxidation. (2) The great conductivity can retain the high electron mobility of BP. Furthermore, the conjugated polymer is a commonly used material in field-effect transistors and organic solar cells, which extends the application areas of composed hybrid materials.[29,30] In this work, we employ a light-absorbing conjugated polymer as the coating material to suppress the ambient degradability of BP (Scheme 1). Light-absorbing polymer coated BP (BP/polymer) is obtained by exfoliating bulk BP in a conjugated polymer containing *N*-methyl pyrrolidone (NMP) solution. The stability of BP/polymer is greatly enhanced under sunlight. Systematic characterization reveals that the crystal structure and electronic characteristics of BP are retained after exposure under sunlight for 30 days.

Experimental section

Materials

Red phosphorus (RP), tin (Sn), tin iodide (SnI_4), methyltrioctylammonium chloride, and 4,7-bis(4,4,5,5-tetramethyl-1,3,2-dioxaborolan-2-yl)-2,1,3-benzothiadiazole were purchased from Aladdin (Shanghai, China). Tetrakis(triphenylphosphine) palladium, perylene-3,4,9,10-tetracarboxylic dianhydride, and 2-ethylhexylamine were purchased from J&K (Beijing, China). Sulfuric acid (H_2SO_4), normal-butanol (*n*-BuOH), and iodine (I_2) were purchased from XiLong SCIENTIFIC (Guangdong, China). Bromine (Br_2), hydrochloric acid (HCl), silica gel, magnesium sulphate ($MgSO_4$), and other chemicals were purchased from Sinopharm Chemical Reagent (Shanghai, China). All chemicals were used without further purification.

Synthesis of bulk BP

Bulk BP was synthesized according to the literature.[7] In detail, 500 mg of RP, 20 mg of Sn, and 10 mg of SnI_4 were sealed in a quartz tube. The tube was heated to 650 °C with a heating ramp rate of about 1.35 °C per min and then cooled down naturally.

Synthesis of BP/polymer

BP/polymer was prepared using a simple liquid exfoliation technique in the polymer/NMP solution. In brief, 100 mg of bulk BP was first ground for 10 min. The powder was added into the polymer/NMP solution (50 mL 1 mg mL^{-1}). Then the mixture was treated by sonication with an ice bath for 24 h. The resultant brown suspension was centrifuged at 1000 rpm for 20 min to remove the residual unexfoliated BP, and the supernatant was centrifuged at 12 000 rpm for 20 min to obtain BP/polymer nanosheets.

Stability measurements

The stability of the samples was investigated *via* a polarizing microscope, transmission electron microscope (TEM), and X-ray photoelectron spectrometer (XPS). Micro-sized BP (from the sediment after sonication with an ice bath for 24 h) was dropped on a glass slide, and then the change of surface morphology was observed *via* a polarizing microscope. Nano-sized BP (from the supernatant after sonication with an ice bath for 24 h) was dropped on the silicon substrate, and then the peak of P and the other peak of P_xO_y were observed *via* an XPS. In an ethanol solution, the stability of micro-sized BP (8000 rpm) was investigated *via* a TEM. During the photothermal stability characterization, a 1 cm path length quartz cuvette containing 1 mL of the samples (20 ppm) was used. An 808 nm NIR laser (Hi-Tech Optoelectronic Technology Co., Ltd.) was employed as a continuous light source with a power density of 1.0 W cm^{-2}, and the temperature change was monitored with a Fotric 220.

Conductivity measurements

Conductivity measurements of BP and BP/Polymer were conducted as follows: the ethanol solution of the samples was dropped onto the glass substrates and dried in a vacuum at 60 °C for 1 h. Then, the current–voltage curves of the samples were measured *via* cyclic voltammetry using a CHI440C (initial E (V) = −1, high E (V) = 1, low E (V) = −1, scan rate (V s^{-1}) = 0.1, sensitivity (A V^{-1}) = 1×10^{-5}).

Characterization

The micrographs of the samples were taken with a TEM (JEOL JEM-2100), high resolution TEM (HRTEM, TECNAI F-30), transmission-reflecting polarizing microscope (ECLIPSE/Ci-S, Nikon), and scanning electron microscope (SEM, SU70, Hitachi). Atomic force microscopy (AFM) images were recorded using an atomic force microscope (AFM, DI Multimode V/DI Multimode V, Veeco) in tapping mode. X-ray diffraction (XRD) patterns were recorded with a Philips X'Pert pro equipped with a Cu Kα radiation source (λ = 1.542 Å) The diffraction pattern was scanned with a step size of 0.02° and a scan speed of 0.2 s per step. The optical properties of the BP nanosheets were characterized with a UV-visible spectrophotometer (UV-2550, Shimadzu). X-ray photoelectron spectroscopy (XPS) measurements were performed on a PHI Quantum 2000 (USA). Fourier transform infrared spectroscopy (FTIR) was performed using

a NICOLET iS10, and Raman spectra (XploRA, Jobin-Yvon) were recorded with a solid-state laser at the excitation wavelength of 532 nm.

Results and discussion

First, bulk BP was prepared and characterized according to a previous report (Fig. S1†).[7] The layered structure of the bulk BP is observed from the scanning electron microscope (SEM) image (Fig. S1a†). X-ray diffraction (XRD) measurements (Fig. S1b†) confirm the well-crystallized structure of the obtained bulk BP (JCPDS no. 73-1358). The conjugated polymer was synthesized by Suzuki coupling polymerization (Fig. S2†). Afterwards, the BP/polymer was obtained by sonication associated liquid-exfoliation in the polymer/NMP solution. As shown in Fig. 1a, BP/polymer has a typical 2D structure with an average size of about 560 nm. The high-resolution transmission electron microscopy (HRTEM) image reveals a lattice spacing of 0.26 nm, which is assigned to the (040) plane of BP. Such observations are similar to the as-prepared BP (Fig. S3†), which indicates that the polymer on BP has no effect on the structure of BP. Energy-dispersive X-ray spectroscopy (EDS) of BP/polymer demonstrates uniform distributions of P, C, N, and O elements on the BP surface (Fig. 1c), confirming the successful functionalization of the conjugated polymer. The average thicknesses of BP and BP/polymer are ~3.35 nm and ~5.30 nm according to the atomic force microscopy (AFM) results, revealing that the thickness of the conjugated polymer coating is ~1 nm (Fig. 1d and S4a†). Moreover, the thickness of the BP/polymer remains unchanged when the amount of polymer is doubled in the synthesis process (Fig. S4b†), which also proves the achievement of maximum functionalization.

The formation of BP/polymer is verified by Fourier transform infrared spectroscopy (FTIR). A weak characteristic band at ~1632.6 cm^{-1} in FTIR of BP is ascribed to H–O–H bending of surface adsorbed water (Fig. 2a).[7] For BP/polymer, the sharp bands observed at ~1705.5 and ~1342.4 cm^{-1} are assigned to the stretching vibration of C=O (as labeled by the circle).[31] The characteristic bands at 1662.2 and 817.1 cm^{-1} arise from the stretching of C=N (as labeled by the pentacle).[32] The other characteristic bands at 1596.7 and 1247.4 cm^{-1} are attributed to the stretching of C=C (as labeled by the triangle) and C–N (as labeled by the inverted pentacle), respectively.[32] Such characteristic bands are consistent with the bands of the conjugated polymer. The ^1H NMR spectra also confirm that the conjugated polymer is successfully adsorbed on the BP surface (Fig. S5†). X-ray photoelectron spectroscopy (XPS) analysis is carried out to assess the chemical states of BP/polymer (Fig. 2b). Full-scan XPS spectra of BP/polymer demonstrate the presence of the relevant elements: P, C, N, and O (Fig. S6†), in agreement with the previous result in EDS mapping. As presented in Fig. 3b, in the high-resolution C 1s XPS spectrum of BP/Polymer, the peaks observed at 284.6, 285.5, 286.2, 287.0, and 288.9 eV are assigned to the C=C, C–N, C=N, C–O, and C=O bonds, respectively.[32–34] The asymmetric peak of N 1s is composed of two peaks, corresponding to the peak of C=N at 398.5 eV and C–N at 400.2 eV (Fig. 2c).[32] The O 1s spectrum (Fig. 2d) exhibits three characteristic peaks at 530.8, 531.8, and 532.9 eV, attributed to C=O, C–O and H_2O, respectively.[33] These results confirm the presence of the conjugated polymer and its successful coating on the BP surface, which is consistent with the FTIR results as discussed.

The structure and conductivity of BP and BP/Polymer are then investigated by Raman spectroscopy, XRD, and conductivity measurements. In Fig. 3a, both BP and BP/polymer show three prominent Raman peaks ascribed to one out-of-plane phonon mode at 361.9 cm^{-1} (A_g^1), and two in-plane modes at 438.8 and 466.9 cm^{-1} (B_{2g} and A_g^2). The ratio of A_g^1/A_g^2 intensity of BP and BP/Polymer is calculated as 0.63 and 0.62, respectively,

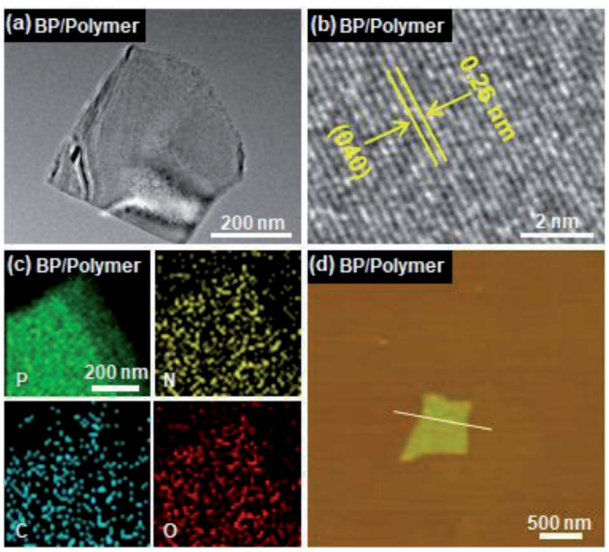

Fig. 1 (a) TEM, (b) high-resolution TEM, (c) elemental mapping, and (d) AFM images of BP/polymer. Inset in (d) is the height profile along the white line.

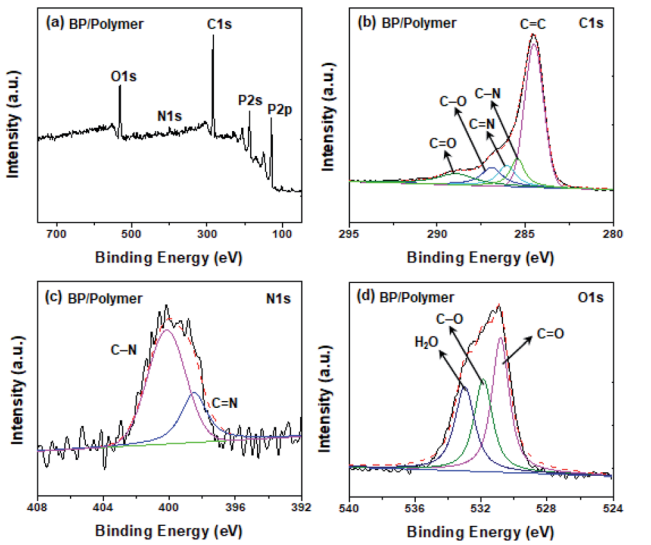

Fig. 2 (a) FTIR spectra of BP, the conjugated polymer, and BP/polymer. High-resolution XPS spectra of (b) C 1s peaks, (c) N 1s peaks, and (d) the O 1s peak of BP/polymer.

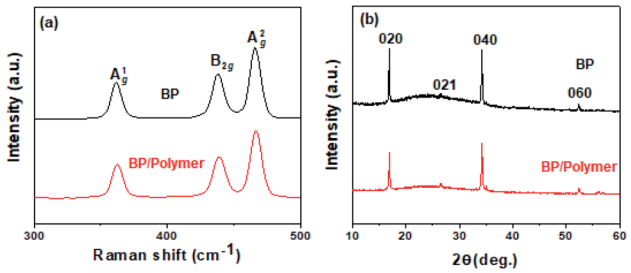

Fig. 3 (a) Raman spectra and (b) XRD patterns of BP and BP/polymer.

suggesting that the basal planes of P remain unoxidized after polymer coating. In Fig. 3b, the XRD pattern of BP/polymer retains the distinctive few-layered BP peaks, indicating the unchanged crystal structure. The resistance of the original BP is measured to be $\sim 0.92 \times 10^5$ Ω (Fig. 3c). Attributed to the intrinsic conductivity of the conjugated polymer, the resistance of conjugated polymer coated BP ($\sim 0.78 \times 10^5$ Ω) does not increase significantly. Overall, according to these results, the surface modification with the conjugated polymer has no influence on the 2D structure and electrical performance of BP nanosheets.

To evaluate the effect of conjugated polymer functionalization on the stability of BP, both nano-sized and micro-sized BP/polymer samples were investigated with a camera, polarizing microscope, TEM and XPS. Firstly, the BP/polymer and BP dispersion with the same concentration (20 ppm) were exposed to sunlight for days and the appearance changes were recorded. As shown in Fig. S8,† after 12 days, the dispersion of bare BP becomes transparent, while that of BP/polymer remains brown, indicating that the BP/polymer has excellent stability in water. Then BP and BP/polymer samples were dropped onto SiO_2 substrates with exposure to a direct sunlight environment for different durations. As presented in Fig. 4, the optical images of micro-sized BP and BP/polymer show a perfectly clean and flat surface at the initial stage. Correspondingly, the same 2D structures with no apparent defects are observed in TEM images (inset of Fig. 4a_1 and b_1). After 3 days of natural light exposure, bubble-like features appear on the micro-sized BP surface (Fig. 4a_2). When the exposure time is extended to 5 days, the "bubbles" on the BP surface become denser and rougher (Fig. 4a_3). Similarly, the BP nanosheets also show "bubbles" obviously after 3 days (inset of Fig. 4a_2) and cannot retain the 2D morphology after 5 days (inset of Fig. 4a_3). In general, both micro-sized and nano-sized BP will undergo severe oxidation and degradation under sunlight. By contrast, the BP/polymer retains its original surface morphology even after exposure in the sunlight for 30 days, which is observed under both the polarizing microscope and TEM (Fig. 4b_3). These results show that the conjugated polymer coating prevents BP from degradation in the sunlight environment, and this effective method can be extended to BP with different sizes.

XPS is further employed to assess the stability of BP and BP/polymer under the sunlight environment. Degradation of BP is mainly due to the light-induced interaction of oxygen and P,

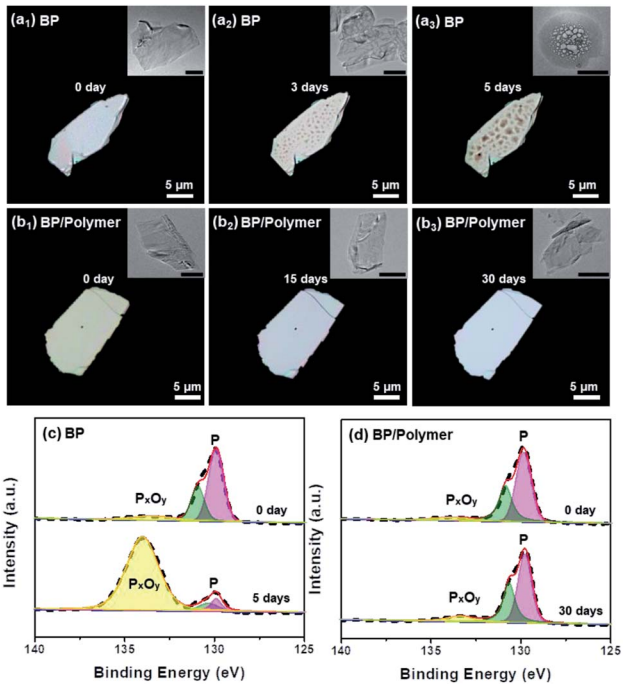

Fig. 4 Polarizing microscopy images of (a) BP and (b) BP/polymer after sunlight exposure for different durations (inset: the corresponding TEM image, scale bar: 200 nm). High-resolution P 2p XPS spectra of (c) BP and (d) BP/polymer after sunlight exposure.

accompanied by the formation of oxidized phosphorus species (BP → P_xO_y).[17] Hence, the evolution process of P_xO_y can provide a more accurate description of the BP surface oxidation degree: with gradual degradation, the content of P_xO_y on the BP surface rises conceivably. Fig. 4c and d display P 2p XPS spectra with P peaks at 128.2–131.7 eV and another peak assigned to P_xO_y at 134.0 eV.[21,35,36] At the initial stage, the spectra of BP and BP/polymer both show a strong P peak and weak P_xO_y peak. After sunlight exposure for 5 days, as for pure BP, the peak intensity of P changes from 92.1% to 14.6% significantly, while the peak intensity of P_xO_y changes from 7.9% to 85.4%, indicating the heavy oxidation of BP (Fig. 4c). In sharp contrast, according to the P 2p spectra of BP/polymer in Fig. 4d, even after 30 days of sunlight exposure, the peak intensity of P has no significant changes (P: from 92.4% to 89.7%), and the peak intensity of P_xO_y slightly increases (P_xO_y: from 7.6% to 10.3%). XPS analysis is consistent with the polarizing microscopy results, suggesting the enhanced ambient stability of BP/polymer over BP under sunlight. This stability improvement enables the use of BP/polymer in a variety of applications in which long-term illumination is essential.

Attributed to the ideal photothermal conversion efficiency and good biocompatibility, BP is regarded as a promising photothermal agent. Thus, bare BP and BP/polymer nanosheets were dispersed in water to evaluate the photothermal stability. As observed from Fig. S9,† bare BP temperature rises by 18 °C with 10 min NIR irradiation at 0 d. However, the heating rate is quickly reduced by 77% accompanied by severe degradation of BP after 9 d. In contrast, the photothermal stability of BP/

Polymer is much better, consistent with environmental stability comparison shown in Fig. 4. After 9 d, the heating rate of the BP/Polymer solution slightly decreases by 10%. It should be noted that the polymer alone shows little photothermal response capability (Fig. S10†). These results indicate that BP/Polymer can maintain photothermal performance for long-term use by environmental stability improvement.

The stability improvement of BP/polymer is attributed to the conjugated polymer, which not only can effectively isolate BP from oxygen and water but also build a light barrier. The light-induced oxidation mechanism demonstrates that reactive oxygen species (ROS) react with BP and form phosphorus oxides, leading to BP degradation. These reactive species are generated by the reaction between oxygen molecules and light excited electrons from the conduction band of BP. And the light-induced oxidation mechanism can be sketched as follows:

Step 1:

$$O_2 + hc/\lambda \xrightarrow{P} O_2^- + h^+ \quad (1)$$

Step 2:

$$O_2^- + P + h^+ \rightarrow P_xO_y \quad (2)$$

where O_2^- is ROS, h is the Planck constant, λ is the wavelength, P is phosphorene, and h^+ and P_xO_y stand for a hole and phosphorus oxides.

As shown in Fig. 5, BP (dispersed in ethanol) exhibits broad absorption from 200 nm to 800 nm. According to the above equations, continuous visible and ultraviolet-light will lead to the generation of plenty of ROS on the BP surface and greatly facilitate the degradation of BP. The conjugated polymer dispersed in ethanol exhibits two kinds of strong absorption peaks: one at ~215 nm, and the other at ~523 nm. Correspondingly, only two absorption peaks are observed in the BP/polymer sample. The absorption peak in the ultraviolet region has a red-shift from ~215 nm to ~239 nm, which is caused by the $\pi \rightarrow \pi^*$ transition of C=C in the BP/polymer sample.[37] Therefore, as the band of wavelength narrowed down, most light absorption at different wavelengths from 200 nm to 800 nm is resisted under the same white light. Without enough photon energy, it is difficult for BP to produce light-induced excitons in Step 1. Thus, the electron transfer process will be significantly hindered or even not occur, which contributes to the ROS reduction and BP stability improvement.

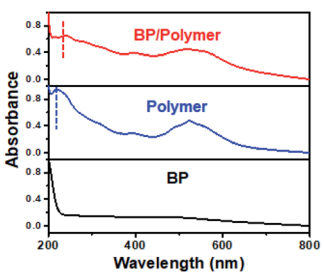

Fig. 5 UV-vis spectra of BP, polymer, and BP/polymer.

Conclusions

In conclusion, light-absorbing conjugated polymer coated BP is produced during the process of exfoliation of bulk BP in the polymer/NMP solution. The successful synthesis for BP/polymer nanosheets is confirmed by the FTIR, ^{1}H NMR, and XPS assessment. The conjugated polymer coating layer on the BP surface shows strong light absorption properties (ultraviolet and visible region), which can serve as a light barrier to avoid photo-oxidative damage on the BP surface. In contrast to rapid degradation of BP, BP/polymer nanosheets demonstrate excellent stability under sunlight in an ambient environment. Our findings provide a simple and efficient strategy to enhance the stability of BP against photo-oxidative degradation, which is of great importance for facilitating future practical applications in nanoelectronics and optoelectronics.

Conflicts of interest

There are no conflicts to declare.

Acknowledgements

This study was financially supported by the National Natural Science Foundation of China (21771154) and the Shenzhen Fundamental Research Programs (JCYJ20190809161013453).

Notes and references

1 L. Li, Y. Yu, G. J. Ye, Q. Ge, X. Ou, H. Wu, D. Feng, X. H. Chen and Y. Zhang, *Nat. Nanotechnol.*, 2014, **9**, 372–377.
2 F. Xia, H. Wang and Y. Jia, *Nat. Commun.*, 2014, **5**, 4458.
3 A. K. Geim, *Science*, 2009, **324**, 1530–1534.
4 Q. H. Wang, K. Kalantar-Zadeh, A. Kis, J. N. Coleman and M. S. Strano, *Nat. Nanotechnol.*, 2012, **7**, 699.
5 Y. Zhao, H. Wang, H. Huang, Q. Xiao, Y. Xu, Z. Guo, H. Xie, J. Shao, Z. Sun, W. Han, X. F. Yu, P. Li and P. K. Chu, *Angew. Chem., Int. Ed.*, 2016, **55**, 5003–5007.
6 P. Yasaei, B. Kumar, T. Foroozan, C. Wang, M. Asadi, D. Tuschel, J. E. Indacochea, R. F. Klie and A. Salehi-Khojin, *Adv. Mater.*, 2015, **27**, 1887–1892.
7 X. Liu, Y. Bai, J. Xu, Q. Xu, L. Xiao, L. Sun, J. Weng and Y. Zhao, *Adv. Sci.*, 2019, 1901991.
8 C. Hao, B. Yang, F. Wen, J. Xiang, L. Li, W. Wang, Z. Zeng, B. Xu, Z. Zhao, Z. Liu and Y. Tian, *Adv. Mater.*, 2016, **28**, 3194–3201.
9 Z. Guo, S. Chen, Z. Wang, Z. Yang, F. Liu, Y. Xu, J. Wang, Y. Yi, H. Zhang, L. Liao, P. K. Chu and X. F. Yu, *Adv. Mater.*, 2017, **29**, 1703811.
10 D. H. Kwak, H. S. Ra, J. Yang, M. H. Jeong, A. Y. Lee, W. Lee, J. Y. Hwang, J. H. Lee and J. S. Lee, *Small*, 2018, **14**, 1703194.
11 Y. Xu, J. Yuan, L. Fei, X. Wang, Q. Bao, Y. Wang, K. Zhang and Y. Zhang, *Small*, 2016, **12**, 5000–5007.
12 J. Sun, Y. Sun, M. Pasta, G. Zhou, Y. Li, W. Liu, F. Xiong and Y. Cui, *Adv. Mater.*, 2016, **28**, 9797–9803.
13 L. Wu, J. Wang, J. Lu, D. Liu, N. Yang, H. Huang, P. K. Chu and X. F. Yu, *Small*, 2018, **14**, 1801405.

14 C. R. Ryder, J. D. Wood, S. A. Wells, Y. Yang, D. Jariwala, T. J. Marks, G. C. Schatz and M. C. Hersam, *Nat. Chem.*, 2016, **8**, 597–602.
15 D. Hanlon, C. Backes, E. Doherty, C. S. Cucinotta, N. C. Berner, C. Boland, K. Lee, A. Harvey, P. Lynch, Z. Gholamvand, S. Zhang, K. Wang, G. Moynihan, A. Pokle, Q. M. Ramasse, N. McEvoy, W. J. Blau, J. Wang, G. Abellan, F. Hauke, A. Hirsch, S. Sanvito, D. D. O'Regan, G. S. Duesberg, V. Nicolosi and J. N. Coleman, *Nat. Commun.*, 2015, **6**, 1–11.
16 Y. Huang, J. Qiao, K. He, S. Bliznakov, E. Sutter, X. Chen, D. Luo, F. Meng, D. Su, J. Decker, W. Ji, R. S. Ruoff and P. Sutter, *Chem. Mater.*, 2016, **28**, 8330–8339.
17 Q. Zhou, Q. Chen, Y. Tong and J. Wang, *Angew. Chem., Int. Ed.*, 2016, **55**, 11437–11441.
18 A. Favron, E. Gaufrès, F. Fossard, A. L. Phaneuf-L'Heureux, N. Y. W. Tang, P. L. Lévesque, A. Loiseau, R. Leonelli, S. Francoeur and R. Martel, *Nat. Mater.*, 2015, **14**, 826–832.
19 G. Abellan, S. Wild, V. Lloret, N. Scheuschner, R. Gillen, U. Mundloch, J. Maultzsch, M. Varela, F. Hauke and A. Hirsch, *J. Am. Chem. Soc.*, 2017, **139**, 10432–10440.
20 H. Wang, S. Jiang, W. Shao, X. Zhang, S. Chen, X. Sun, Q. Zhang, Y. Luo and Y. Xie, *J. Am. Chem. Soc.*, 2018, **140**, 3474–3480.
21 Y. Cao, X. Tian, J. Gu, B. Liu, B. Zhang, S. Song, F. Fan and Y. Chen, *Angew. Chem., Int. Ed.*, 2018, **57**, 4543–4548.
22 H. Hu, H. Gao, L. Gao, F. Li, N. Xu, X. Long, Y. Hu, J. Jin and J. Ma, *Nanoscale*, 2018, **10**, 5834–5839.
23 X. Jiang, H. Jin and R. Gui, *Dalton Trans.*, 2020, **49**, 11911–11920.
24 X. Jiang, H. Jin and R. Gui, *Biosens. Bioelectron.*, 2020, **165**, 112390.
25 J. D. Wood, S. A. Wells, D. Jariwala, K. S. Chen, E. Cho, V. K. Sangwan, X. Liu, L. J. Lauhon, T. J. Marks and M. C. Hersam, *Nano Lett.*, 2014, **14**, 6964–6970.
26 B. Wan, B. Yang, Y. Wang, J. Zhang, Z. Zeng, Z. Liu and W. Wang, *Nanotechnology*, 2015, **26**, 435702.
27 J. Kang, D. Jariwala, C. R. Ryder, S. A. Wells, Y. Choi, E. Hwang, J. H. Cho, T. J. Marks and M. C. Hersam, *Nano Lett.*, 2016, **16**, 2580–2585.
28 D. Baran, A. Balan, S. Celebi, B. Meana Esteban, H. Neugebauer, N. S. Sariciftci and L. Toppare, *Chem. Mater.*, 2010, **22**, 2978–2987.
29 E. Wang, W. Mammo and M. R. Andersson, *Adv. Mater.*, 2014, **26**, 1801–1826.
30 O. Knopfmacher, M. L. Hammock, A. L. Appleton, G. Schwartz, J. Mei, T. Lei, J. Pei and Z. Bao, *Nat. Commun.*, 2014, **5**, 1–9.
31 T. Yang, Y. Cui, Z. Li, H. Zeng, S. Luo and W. Li, *J. Hazard. Mater.*, 2018, **357**, 475–482.
32 B. Yuan, C. Bao, L. Song, N. Hong, K. M. Liew and Y. Hu, *Chem. Eng. J.*, 2014, **237**, 411–420.
33 H. Miao, J. Yang, Y. Wei, W. Li and Y. Zhu, *Appl. Catal., B*, 2018, **239**, 61–67.
34 Q. Su, S. Pang, V. Alijani, C. Li, X. Feng and K. J. A. m. Müllen, *Adv. Mater.*, 2009, **21**, 3191–3195.
35 M. Qiu, D. Wang, W. Liang, L. Liu, Y. Zhang, X. Chen, D. K. Sang, C. Xing, Z. Li, B. Dong, F. Xing, D. Fan, S. Bao, H. Zhang and Y. Cao, *Proc. Natl. Acad. Sci. U. S. A.*, 2018, **115**, 501–506.
36 Z. Sun, H. Xie, S. Tang, X. F. Yu, Z. Guo, J. Shao, H. Zhang, H. Huang, H. Wang and P. K. Chu, *Angew. Chem., Int. Ed.*, 2015, **54**, 11526–11530.
37 S. J. Chen, Q. Y. Zhang, H. P. Zhang, J. W. Gu, M. L. Ma, T. J. Xin, Y. Y. Zhou, J. Zhou and Q. Liu, *Polym. Chem.*, 2012, **3**, 2244–2253.